Characterization of A Practical 3-m VLC System Using Commercially Available Tx/Rx Modules

Chen Chen[1,*], Yungui Nie[1], Xin Zhong[1], Min Liu[1], and Binbin Zhu[2]
[1]*School of Microelectronics and Communication Engineering, Chongqing University, Chongqing 400044, China*
[2]*Shenzhen Hua Chuang Chip Lighting Co., Ltd, Shenzhen 518027, China*
c.chen@cqu.edu.cn

Abstract: We experimentally characterize the performance of a practical 3-m VLC system using commercially available Tx/Rx modules. Results show that the achievable rates are at least 120 and 320 Mbit/s when applying OOK and OFDM, respectively. © 2021 The Author(s)

1. Introduction

As an emerging technology enabled by the worldwide deployment of light-emitting diodes (LEDs) for general lighting, visible light communication (VLC) employing commercial off-the-shelf LEDs has attracted great attention from both academia and industry in recent years [1]. As the downlink communication technology of light-fidelity (LiFi) networks, VLC has been recognized as the key enabler for 6G and Internet of Things (IoT) communication [2-4]. In comparison to traditional radio frequency (RF) communication technology, VLC enjoys many advantages such as simultaneous lighting and communication, abundant unregulated spectrum, inherent physical-layer security and no electromagnetic interference emission [5]. In typical VLC systems, the transmitter (Tx) part generally includes LED driver, LED source and transmitter optics, while the receiver (Rx) part mainly consists of receiver optics, photo-detector (PD) and amplifier [6,7]. State-of-the-art experimental VLC systems reported in the literature show the potential to achieve Gbit/s and even tens of Gbit/s data rates by using large-bandwidth LEDs [8], demonstrating the promising future of VLC for high-speed short-reach wireless communications. Nevertheless, current experimental VLC systems are basically built upon multiple discrete optical and electrical components, and such systems are still far away from practical implementation and deployment in real-world applications. Towards the commercialization of the promising VLC technology, system and component integration is a vital step that should be taken. Lately, a few integrated Tx and Rx modules have been designed and commercialized by pioneering domestic and overseas VLC companies.

In this paper, for the first time to the best of our knowledge, we experimentally characterize the performance of a practical 3-m VLC system using a pair of commercially available Tx and Rx modules. The performance of the blue mini-LED adopted in the Tx module is first characterized and then the electrical-optical-electrical (EOE) frequency response of the system is measured. After that, the transmission performance of the system using both on-off-keying (OOK) and orthogonal frequency division multiplexing (OFDM) modulation is further characterized.

2. Practical 3-m VLC system using Tx/Rx modules

Fig. 1 depicts the photos the Tx module and the Rx module employed in the practical 3-m VLC system, respectively. As we can see, the Tx module (HCCLS2021MOD01-TX) has two connectors, corresponding to the DC and AC ports, respectively. The voltage applied on the DC input is set as 12 V so as to supply the DC driven current for the internal components such as the LED transmitter and signal amplifier. The analog signal to be transmitted in the VLC system is input through the AC port of the Tx module, and the default peak-to-peak voltage of the AC input is 250 mV. The input voltage signal is converted to a current signal in the Tx module, and hence the adverse effect of LED nonlinearity during direct voltage modulation of LED transmitter can be minimized. Driven by both DC and AC signals, the Tx module radiates light from an embedded blue mini-LED (HCCLS2021CHI03), which has an emission wavelength of 459.3 nm, an optical power of 18.5 mW and a small-signal -3dB bandwidth of about 90 MHz. The size of the generated light spot can be adaptively adjusted by the optical collimator lens employed in the Tx module.

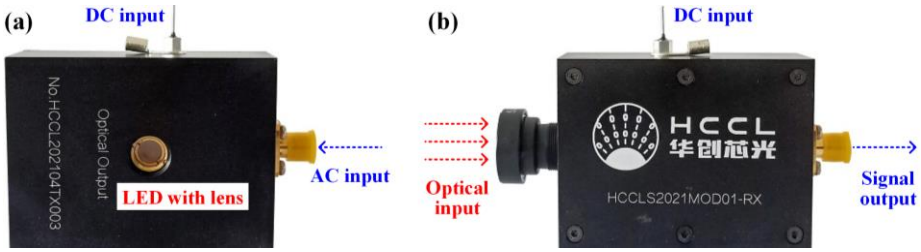

Fig. 1. Photos of (a) the Tx module and (b) the Rx module.

Moreover, the Rx module (HCCLS2021MOD01-RX) is also driven by a 12-V voltage applied on the DC port. The light radiated from the Tx module is captured by a large-area PIN detector embedded in the optical input part of the Rx module. A combination of two optical lenses is employed in front of the PIN detector to ensure a long transmission distance. The photocurrent generated by the PIN detector is amplified by the transimpedance and voltage amplifiers, and the resultant electrical signal is then output through the output port of the Rx module for digital demodulation.

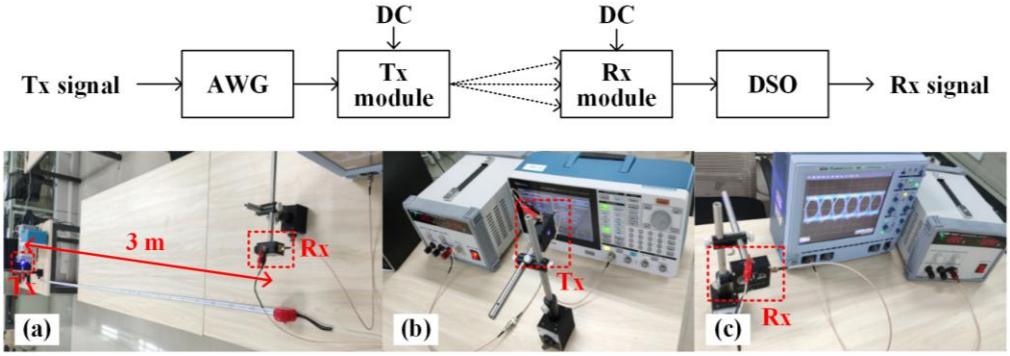

Fig. 2. Experimental setup of the 3-m VLC system using a pair of commercially available Tx and Rx modules. Insets: photos of (a) the overall system, (b) the Tx side and (c) the Rx side.

Fig. 2 shows the experimental setup of the 3-m VLC system using the Tx and Rx modules. As can be seen, the Tx side includes the Tx module, a DC supply and an arbitrary waveform generator (AWG, Tektronix AFG31102), while the Rx side includes the Rx module, a DC supply and a digital storage oscilloscope (DSO, LeCroy WaveSurfer 432). The photos of the overall system, the Tx side and the Rx side are depicted in the insets (a), (b) and (c), respectively.

3. Performance characterization

In the next, we characterize the performance of the practical 3-m VLC system using the Tx and Rx modules. First, we present the performance of the blue mini-LED adopted in the Tx module. Fig. 3(a) shows the measured I-V curve of the blue mini-LED. As we can observe, the current increases slowly with the increase of voltage when the voltage is in the range of 3.1 to 3.4 V, while a rapid increase of the current occurs when the voltage is in the range of 3.4 to 3.45 V. The corresponding P-I curve is plotted in Fig. 3(b). It can be found from Figs. 3(a) and (b) that the LED exhibits certain nonlinearity and the available linear dynamin range is within 80 to 140 mA. Hence, the optimal DC bias current of the LED can be set to 110 mA, which is the default DC bias current adopted in the Tx module. Fig. 3(c) shows the measured EOE frequency response of the overall system using the Tx/Rx modules through the OFDM-based channel estimation approach. Clearly, the overall system has a typical low-pass frequency response, and the measured -3dB bandwidth is about 63.5 MHz.

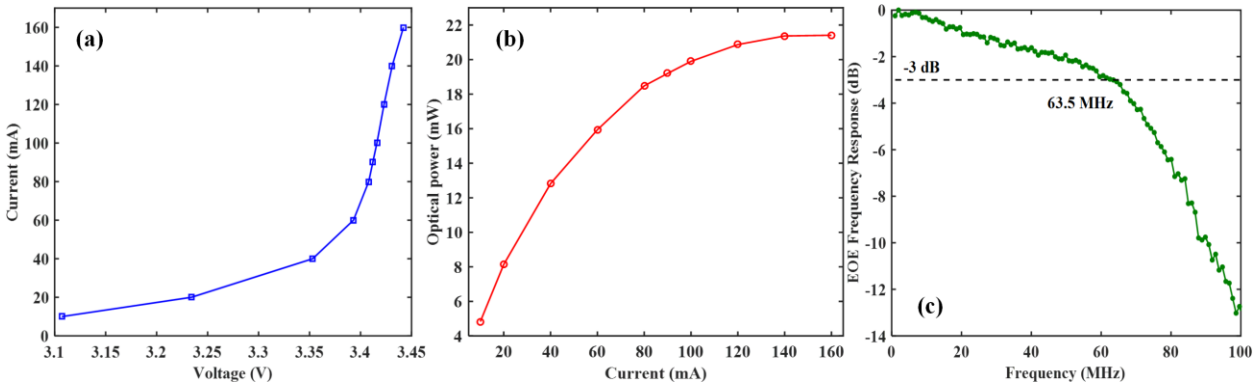

Fig. 3. Measured (a) I-V and (b) P-I curves of the blue mini-LED used in the Tx module, and (c) the EOE frequency response of the overall system using Tx/Rx modules.

After that, we evaluate the transmission performance of the practical 3-m VLC system using the Tx and Rx modules, where two types of modulation schemes, i.e., OOK and OFDM, are considered. For both OOK and OFDM modulation, the signals are generated offline via MATLAB and then uploaded to the AWG for digital-to-analog conversion (DAC). For OOK modulation, the data rate of OOK signals can be adjusted by changing the sampling rate of the AWG. In the

evaluation, OOK signals with four different data rates, i.e., 60, 80, 100 and 120 Mbit/s, are transmitted in the system. Fig. 4(a) depicts the measured eye diagrams of the received four different OOK signals. For the data rate of 60 Mbit/s, the OOK signal has a clear and wide-open eye diagram. When the data rate is increased from 60 to 120 Mbit/s, the eye diagrams of the OOK signals become less clear and the eyes are gradually closed. Nevertheless, for all the four data rates, the bit error rates (BERs) of the OOK signals are all zero, indicating that a data rate of at least 120 Mbit/s can be achieved by the system applying simple OOK modulation.

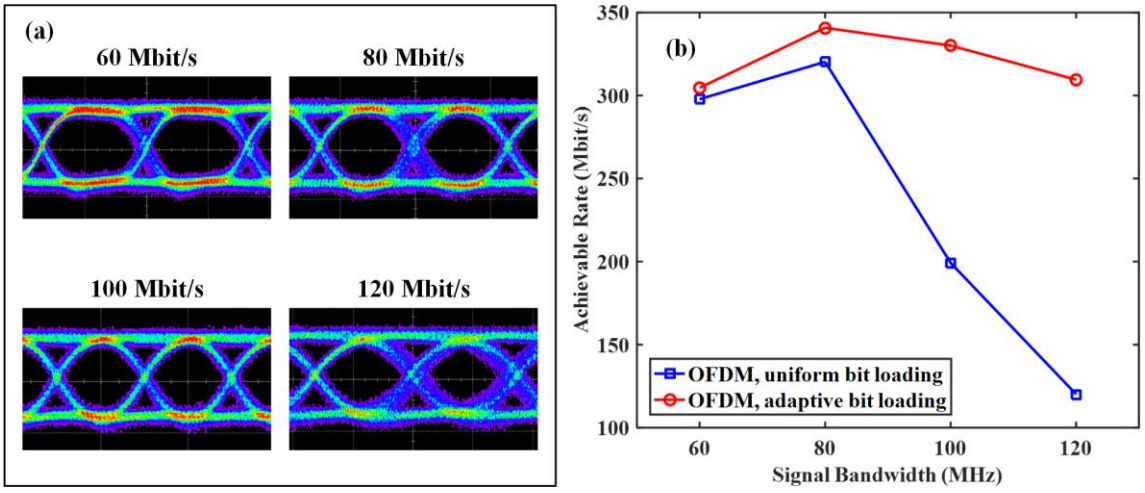

Fig. 4. (a) Eye diagrams of OOK signals and (b) achievable rate vs. signal bandwidth for OFDM signals.

Furthermore, for OFDM modulation, we consider two bit-loading approaches: one is uniform bit loading and the other is adaptive bit loading. We evaluate the achievable rate of OFDM modulation using both uniform and adaptive bit loading approaches under various signal bandwidths. The bandwidth of OFDM signals can be dynamically adjusted by varying the number of subcarriers for data transmission during OFDM modulation [9]. The achievable rate versus signal bandwidth is shown in Fig. 4(b), where four signal bandwidths of 60, 80, 100 and 120 MHz are considered. For OFDM with uniform bit loading, the achievable rate first increases when the signal bandwidth is increased from 60 to 80 MHz, and then decreases rapidly with the further increase of the signal bandwidth. Specifically, a maximum rate of 320.3 Mbit/s is obtained with the signal bandwidth of 80 MHz. For OFDM with adaptive bit loading, the achievable rate also first increases and then decreases with the increase of signal bandwidth from 60 to 120 MHz. Differing from OFDM with uniform bit loading, the achievable rate for OFDM with adaptive bit loading is slowly decreased when the signal bandwidth is increased from 80 to 120 MHz. The maximum rate for OFDM with adaptive bit loading is 340.8 Mbit/s, which is also achieved with the signal bandwidth of 80 MHz. According to Fig. 4(b), we can conclude that there exists an optimal signal bandwidth to achieve the maximum rate for OFDM modulation with both uniform and adaptive bit loading. Therefore, the practical 3-m VLC system using the Tx and Rx modules can achieve at least 120 Mbit/s data rate when adopting simple OOK modulation and more than 320 Mbit/s when using OFDM modulation.

4. Conclusion

In this paper, we have experimentally characterized the performance of a practical 3-m VLC system using a pair of commercially available Tx and Rx modules. Specifically, the overall system exhibits a relatively large -3dB bandwidth is about 63.5 MHz. Experimental results show that the achievable data rates of the practical 3-m VLC system using the Tx and Rx modules are more than 120 and 320 Mbit/s, when applying OOK and OFDM modulation, respectively.

5. References

[1] L. Grobe, et al., "High-speed visible light communication systems," IEEE Commun. Mag. **51**(12), 60–66 (2013).
[2] N. Chi, et al., "Visible light communication in 6G: Advances, challenges, and prospects," IEEE Veh. Technol. Mag., **15**(4), 93–102 (2020).
[3] I. Demirkol, et al, "Powering the Internet of Things through light communication," IEEE Commun. Mag. **57**(6), 107–113 (2019).
[4] C. Chen, et al., "NOMA for energy-efficient LiFi-enabled bidirectional IoT communication," IEEE Trans. Commun. **69**(3), 1693–1706 (2021).
[5] H. Haas, "Visible light communication," in OFC 2015, Paper Tu2G.5.
[6] S. Rajbhandari, et al., "High-speed integrated visible light communication system: Device constraints and design considerations," IEEE J. Sel. Areas Commun. **33**(9), 1750–1757 (2015).
[7] Y. Zhang, et al., "Recent advances in the hardware of visible light communication," IEEE Access **7**, 91093–91104 (2019).
[8] R. Bian, et al., "15.73 Gb/s visible light communication with off-the-shelf LEDs," J. Lightw. Technol. **37**(10), 2418–2424 (2019).
[9] C. Chen, et al., "Indoor OFDM visible light communications employing adaptive digital pre-frequency domain equalization," in CLEO 2016, Paper JTh2A.118.